# Noise PDF Analysis of Nonlinear Image Sensor Model: GOCI Case

Myung, Hwan-Chun
Korea Aerospace Research Institute
Email: mhc@kari.re.kr

Youn, Heong-Sik
Korea Aerospace Research Institute
Email: youn@kari.re.kr

*Abstract*— **The paper clarifies all the noise sources of a CMOS image sensor, with which the GOCI (Geostationary Ocean Color Imager) is equipped, and analyzes their contribution to a nonlinear image sensor model. In particular, the noise PDF (Probability Density Function) is derived in terms of sensor-gain coefficients: a linear and a nonlinear gains. As a result, the relation between the noise characteristic and the sensor gains is studied.**

**Key Words:** Noise PDF, Nonlinear Image Sensor Model, GOCI

## I. Introduction

The GOCI (Geostationary Ocean Color Imager) is successfully being developed so far and currently scheduled to be launched through the COMS (Communication, Ocean, Meteorological Satellite) program in 2009. As the rst geostationary ocean imager, it is designed with the CMOS detector (1414x1430), differently from the CCD detector widely used in the LEO (Low Earth Orbit). The CMOS detector shows a nonlinear response due to the saturated photoelectrons. Accordingly, a nonlinear image sensor model is taken into account for the GOCI calibration.

The early research works [1][2][3] have mainly focused on the linear CCD image seonsor model. Even if the CCD noise sensor model shows little big difference from the CMOS one in a nal form, the linearity in the works limits their applicability and provides an approximate result only in a linear region. Another dif culty of the previous research result [1] also represents that the Gaussian feature in a linear noise model vanishes away through the averaging process. It means that the linear noise model cannot re ect the exact effect of the averaging process in a payload.

The paper classi es the noise sources generated from a CMOS image sensor into ve parts: a dark current offset, a shot-noise dependent upon dark electrons and photoelectrons, a read-out noise embedded in a CMOS device and ampli ers, a quantization noise, an electrical offset. All the noise sources are applied to a nonlinear image sensor model ,which comprises a linear and a nonlinear gains, so that the nal noise PDF is induced. The variable related to the gain variables or some independent variable is replaced with a gain-variable function or measured in advance as a priori knowledge, respectively. This leads to the gain-dependent noise PDF which can be used to identify the relation between the gain coef cients and the noise PDF.

Section II clari es the CMOS noise sources and Section III induces the noise PDF applying the noise sources to a nonlinear image sensor model. Some simulation results are included in Section IV to check the properties of the noise PDF. Finally, the concluding remark is given in Section V.

## II. CMOS Noise Sources

The CMOS image sensor generates largely two kinds of noises: temporal and spatial noises [5]. Whereas the former is a result of the time-dependent uctuation limited to each pixel, the latter means the device mismatch among pixels. In a image sensor model, the input-output relation is normally de ned by each pixel and the pixel noise is a main concern for the SNR (Signal to Noise Ratio) issue. That is why the temporal noise sources only are considered in the paper.

The temporal noise sources generally stems from ve different parts [5]. They are a dark current offset ($O_D$), a shot noise ($N_S$), a read-out noise ($N_R$), a quantization noise ($N_Q$), and an electrical offset ($O_E$). $O_D$ is the number of thermally generated electrons due to the dark current, which is independent of input-photoelectrons and heavily depends on the temperature. As a signal offset, $O_D$ still remains included in the nal video signal even after the averaging process. $N_S$ has a zero mean Poisson distribution whose variance depends on two different things: dark electrons and input-photoelectrons. It normally happens by the random arrival of electrons in the detector. The arrival of electrons in a given period is well known to be governed by a Poisson distribution. Moreover, its large variance allows a poisson distribution to be approximated by a Gaussian distribution [4]. Assuming the high input irradiance in a image sensor model is so reasonable that a Gaussian distribution replaces a Poisson distribution for the shot noise n the section III. $N_R$ indicates the composition of a pixel reset noise and a CMOS device noise. The pixel reset noise is measured as the uncertainty of the reset level when the input signal is acquired relative to it. The CMOS device noise is associated with the sampling process and, the built-in and the programmable ampli cation. All the read-out noise sources are commonly associated with the thermal noise. Recently, the advanced methods such as a band-pass lter , a unidirectional swtich, etc. are fabricated to reduce the effect of the read-out noise by transforming a white noise into a color noise. For that reason, the read-out noise distribution is justi ably assumed to be a zero mean Gaussian distribution in the section III. An analog to

digital conversion for a digital image quantizes an analog signal from the CMOS detector. The quantization process results in $N_Q$ as another image sensor noise. In general, the quantization noise is modeled in a form of the zero mean uniform distribution over the range $[-\frac{q}{2}, \frac{q}{2}]$ with the variance $\frac{q^2}{12}$, in which $q$ is the quantization step [1]. Finally, as the other signal offset, the whole electrical path in a CMOS image sensor necessarily entails $O_E$ which is due to the embedded electrical devices such as an amplifier, a buffer, and so on.

## III. Derivation of Noise PDF

In general [6], the number of input electrons ($I$) is given by processing an integration time ($T$ in seconds), an input-spectral irradiance ($X(x, y, \lambda)$ in watt/unit area), and a spatial response ($S(x, y)$), a spectral density efficiency ($R(\lambda)$ in electrons/Joule) such as

$$I_{ij}(\lambda) = T \int_{y(i,j)} \int_{x(i,j)} X(x, y, \lambda) S(x, y) R(\lambda) dx dy, \tag{1}$$

where $i$ and $j$ indicate a pixel position on a detector, and $\lambda$ means the wavelength. Throughout the paper, all the variable related to the image sensor model is defined differently according to the position index and the wavelength. Therefore, for convenience, they will be ruled out without confusion.

Considering the GOCI nonlinear image sensor model [6] and the noise sources, the relation between the input-photoelectrons and the output-digital value ($D$) is

$$D = g_1(I + N_{DSR}) - g_2(I + N_{DSR})^2 + N_{EQ}, \tag{2}$$

in which $g_1(> 0)$ and $g_2(> 0)$ are the linear and the nonlinear gains, respectively, $N_{DSR}$ means the main internal noise variable before the gains, and $N_{EQ}$ refers to the complementary noise variable after the gains. As mentioned in Section II, the noise variables are defined by

$$N_{DSR} = O_D + N_S + N_R, \; N_{EQ} = O_E + N_Q. \tag{3}$$

Then, reformulating the relation with the noise random variables, we obtain the non-stochastic relation

$$D_{av} = g_1(I + O_D) - g_2(I + O_D)^2 + O_E + \overline{D}_N \tag{4}$$

and the stochastic relation

$$D_N = g_1 N_{SR} - g_2 N_{SR}(N_{SR} + 2(I + O_D)) + N_Q, \tag{5}$$

where

$$\overline{D}_N = \mathbf{E}[D_N], \; N_{SR} = N_S + N_R. \tag{6}$$

Rearranging (5) simply results in

$$\begin{aligned} D_N &= (g_1 - 2\mu g_2) N_{SR} - g_2 N_{SR}^2 + N_Q \\ &= \rho N_{SR} - g_2 N_{SR}^2 + N_Q \\ &= N_I + N_Q, \end{aligned} \tag{7}$$

in which

$$\mu = I + O_D, \; \rho = g_1 - 2\mu g_2 \tag{8}$$

and

$$N_I = \rho N_{SR} - g_2 N_{SR}^2. \tag{9}$$

In (4), the meaningful solution of $\mu$, which is associated with the relation between the input-photoelectron and the output digital value, is

$$\mu = \frac{g_1 - \sqrt{{g_1}^2 - 4g_2(D_{av} - O_E - \overline{D}_N)}}{2g_2}, \tag{10}$$

because $\mu$ is inversely proportional to $D_{av}$ with the other one. Accordingly, (10) induces two basic conditions

$$g_1^2 \geq 4g_2(D_{av} - O_E - \overline{D}_N) \tag{11}$$

and

$$\rho = \sqrt{{g_1}^2 - 4g_2(D_{av} - O_E - \overline{D}_N)} \geq 0. \tag{12}$$

For the random variable $N_{SR}$, we assume that the number of the input electrons is very high due to the high optical gain. This reasonable assumption allows the Poisson distribution of $N_S$ to approximate to the Gaussian distribution with the variance of $\mu$. The read-out noise random variable $N_R$ as the composition of the thermal noise sources is assumed to have a zero mean Gaussian distribution and the variance of $\tau^2$. Therefore, $N_{SR}$ becomes the sum of two random variables ($N_S$ and $N_R$). It means that

$$f_{N_{SR}}(x) = \frac{1}{\sqrt{2\pi(\mu + \tau^2)}} e^{-\frac{x^2}{2(\mu+\tau^2)}} = \frac{1}{\sqrt{2\pi\sigma^2}} e^{-\frac{x^2}{2\sigma^2}}, \tag{13}$$

is the PDF of $N_{SR}$. Applying (13) to (9), we can formulate the CDF (Cumulative Distribution Function) of $N_I$

$$F_{N_I}(x) = \frac{1}{\sqrt{2\pi\sigma^2}} \Big( \int_{\psi_1(x)}^{\infty} e^{-\frac{\psi^2}{2\sigma^2}} d\psi + \int_{-\infty}^{\psi_2(x)} e^{-\frac{\psi^2}{2\sigma^2}} d\psi \Big), \tag{14}$$

in which

$$\psi_1(x) = \frac{\rho + \sqrt{\rho^2 - 4g_2 x}}{2g_2}, \; \psi_2(x) = \frac{\rho - \sqrt{\rho^2 - 4g_2 x}}{2g_2} \tag{15}$$

are positive. Here, as another basic condition, (15) entails

$$x < \frac{\rho^2}{4g_2}, \tag{16}$$

which limits the upper bound of $x$. By differentiating (14), the PDF of $N_I$

$$f_{N_I}(x) = \frac{1}{\sqrt{2\pi\sigma^2(\rho^2 - 4g_2 x)}} \Big( e^{-\frac{\psi_1^2(x)}{2\sigma^2}} + e^{-\frac{\psi_2^2(x)}{2\sigma^2}} \Big) \tag{17}$$

is sequentially driven.

Then, we consider the quantization noise $N_Q$, which has the uniform distribution, in order to calculate the PDF of $D_N$. Because $N_I$ and $N_Q$ is independent each other, the

convolution of two PDFs finally generates the noise PDF of the GOCI nonlinear image sensor model

$$f_{D_N}(x) = \int_{-\frac{q}{2}}^{\frac{q}{2}} f_{N_Q}(\tau) f_{N_I}(x-\tau) d\tau$$
$$= \frac{1}{q\sqrt{\pi}} \Big( \int_{\psi_1(x+\frac{q}{2})/\sqrt{2}\sigma}^{\psi_1(x-\frac{q}{2})/\sqrt{2}\sigma} e^{-\eta^2} d\eta - \int_{\psi_2(x+\frac{q}{2})/\sqrt{2}\sigma}^{\psi_2(x-\frac{q}{2})/\sqrt{2}\sigma} e^{-\eta^2} d\eta \Big). \quad (18)$$

Here, we need the modified condition of (16)

$$x \le \frac{\rho^2}{4g_2} - \frac{q}{2}, \; q \neq 0 \quad (19)$$

to assure the convolution procedure in (18). According to the definition of a Gauss error function [7], we find that the result of (18) is obtained in the function

$$f_{D_N}(x) = \frac{1}{2q} \Big( erf\big(\frac{\psi_1(x-\frac{q}{2})}{\sqrt{2}\sigma}\big) - erf\big(\frac{\psi_1(x+\frac{q}{2})}{\sqrt{2}\sigma}\big) - erf\big(\frac{\psi_2(x-\frac{q}{2})}{\sqrt{2}\sigma}\big) + erf\big(\frac{\psi_2(x+\frac{q}{2})}{\sqrt{2}\sigma}\big) \Big). \quad (20)$$

Meanwhile, the PDF of $N_I$ in (17)

$$f_{N_I}(x) = \frac{1}{\sqrt{2\pi\sigma^2(\rho^2 - 4g_2x)}} e^{-\frac{\psi_1^2(x)}{2\sigma^2}} \Big(1 + e^{\frac{4\rho\sqrt{\rho^2-4g_2x}}{8g_2^2\sigma^2}}\Big) \quad (21)$$

is approximately similar to

$$\widetilde{f}_{N_I}(x) = \frac{1}{\sqrt{2\pi\sigma^2(\rho^2 - 4g_2x)}} e^{-\frac{\psi_2^2(x)}{2\sigma^2}}, \quad (22)$$

assuming that

$$\frac{4\rho\sqrt{\rho^2 - 4g_2x}}{8g_2^2\sigma^2} \gg 0. \quad (23)$$

Then, we obtain the approximation of $f_{D_N}(x)$

$$\widetilde{f}_{D_N}(x) = \frac{1}{2q} \Big( erf\big(\frac{\psi_2(x+\frac{q}{2})}{\sqrt{2}\sigma}\big) - erf\big(\frac{\psi_2(x-\frac{q}{2})}{\sqrt{2}\sigma}\big) \Big). \quad (24)$$

Moreover, if the value of $g_2$ converges to 0, (20) becomes

$$\lim_{g_2 \to 0} f_{D_N}(x) = \frac{1}{2q} \Big( erf\big(\frac{x+\frac{q}{2}}{\sqrt{2}\sigma g_1}\big) - erf\big(\frac{x-\frac{q}{2}}{\sqrt{2}\sigma g_1}\big) \Big), \quad (25)$$

which complies with the noise PDF of a linear image sensor model, because

$$\lim_{g_2 \to 0} \psi_1(x) = \infty, \quad \lim_{g_2 \to 0} \psi_2(x) = \frac{x}{g_1}. \quad (26)$$

Since the mean value $\overline{D}_N$ is driven by

$$\overline{D}_N = \mathbf{E}[D_N] = \mathbf{E}[N_I] + \mathbf{E}[N_Q] = \mathbf{E}[N_I]$$
$$(\because \mathbf{E}[N_Q] = 0), \quad (27)$$

we induce the mean value of $N_I$ from (9) in order to obtain $\overline{D}_N$. Reformulating (9) gives

$$N_I = -g_2\sigma^2 \Big( \frac{N_{SR} - \frac{\rho}{2g_2}}{\sigma} \Big)^2 + \frac{\rho^2}{4g_2}$$
$$= -g_2\sigma^2 \widehat{N}_{SR}^2 + \frac{\rho^2}{4g_2}, \quad (28)$$

where $\widehat{N}_{SR}$ is the Gaussian distribution whose mean and variance are $-\frac{\rho}{2g_2\sigma}$ and 1, respectively. By [7], the PDF of $\widehat{N}_{SR}^2$ exactly complies with the $\chi^2$ distribution in one degree of freedom whose mean is $1 + (\frac{\rho}{2g_2\sigma})^2$. Therefore, we find that

$$\overline{D}_N = \mathbf{E}[N_I] = -g_2\sigma^2\big(1 + (\frac{\rho}{2g_2\sigma})^2\big) + \frac{\rho^2}{4g_2} = -g_2\sigma^2. \quad (29)$$

Since $\sigma^2$ is described by $\overline{D}_N$ in (10) and (13), (29) is simultaneously equated with (10) in order to calculate $\overline{D}_N$. The simultaneous equating provides the conditions for the solution such as

$$\overline{D}_N = 0 \;\; \text{if } g_2 = 0, \quad (30)$$

and

$$D_{av} \le \frac{g_1^2}{4g_2} + \frac{g_2}{4} - \frac{g_1}{2} - g_2\tau^2 + O_E \;\; \text{if } g_2 \neq 0. \quad (31)$$

Then, based upon (30) and (31), we select an appropriate solution

$$\overline{D}_N = \frac{\sqrt{g_1^2 + g_2^2 - 2g_1g_2 - 4g_2^2\tau^2 - 4g_2(D_{av} - O_E)}}{2} - \frac{g_1 - g_2 + 2g_2\tau^2}{2}. \quad (32)$$

Accordingly, $\sigma^2$ in (20) can be obtained by inserting (32) in (10), without any knowledge about $\mu$. And we find that applying (31) and (32) to (11) consistently guarantees the condition (11). The variance can be also obtained in the same way. According to [7], the variance of $\widehat{N}_{SR}^2$ is

$$\mathbf{V}[\widehat{N}_{SR}^2] = 2(1 + \frac{\rho^2}{2g_2^2\sigma^2}). \quad (33)$$

Since $N_I$ and $N_Q$ are uncorrelated, we find the variance of $D_N$ as follow:

$$\mathbf{V}[D_N] = \mathbf{V}[N_I] + \mathbf{V}[N_Q]$$
$$= (g_2\sigma^2)^2 \mathbf{V}[\widehat{N}_{SR}^2] + \frac{q^2}{12}$$
$$= 2g_2^2\sigma^4 + \rho^2\sigma^2 + \frac{q^2}{12}. \quad (34)$$

Differently from the other variables, $O_E$ and $\tau^2$ are given by measurement as a priori knowledge. In common, they are effectively acquired during the dark current measurement of the GOCI, which is normally implemented with a dark plate positioned in front of a detector. In particular, (4) can be approximately replaced with a linear image sensor model ($g_2 = 0$) in the low input range such as a dark current. For the reason, two differently integrated

acquisitions are suf cient to separate $O_E$ from the integration time-related $O_D$. Moreover, as the noise measurement of $N_{SR}$ in the low input range is mostly dominated by $N_R$, in comparison to $N_S$ [1], $\tau^2$ is also independently obtainable from the point of view. In consequence, given $D_{av}$, $O_E$, $\tau^2$, and $q$, we can nd the gain-dependent PDF $(f_{D_N}(x)|_{g_1,g_2})$ of a GOCI nonlinear image sensor model as shown in (20).

## IV. Simulation

Here, we properly de ne the values of the variables so that the relation between the PDF and the variables is more clearly noticed, which makes them much larger than the real ones in GOCI.

Fig. 1 shows the characteristic of the PDF in terms of the gain variation. In (a), the PDFs are generated with the different linear gains: 110, 130, 170, 200, and 300. As shown in (a), it is noted that the larger $g_1$ leads to the larger variance. The fact is de nitely expected in (34), which results from the effect of the increased $\rho$ and $\sigma$. Since the $\rho$ is the dominant factor in (34) and in a inverse relation with $g_2$ in (12), the large $g_2$ indicates the small variance in (b). Additionally, we nd the nonsymmetric distortion of the PDF caused by the large $g_2$. As a inverse similarity measure of the Gaussian distribution, the *kurtosis* is calculated in (c) with the respect to $g_1$ and $g_2$. $g_1 = 110$ and $g_2 = 2$ shows the most Gaussian likelihood distribution among the candidates in (c).

Fig. 2 (a) describes the responses of the PDF with the input variation. It is remarked in (b) that the noncentral mean value increases as the $D_{av}$ does. In accordance with (c), we verify that the SNR (Signal-Noise-Ratio) value becomes better with the increased input electrons.

## V. Concluding Remark

The nonlinear image sensor model is used to formulate the noise PDF of the GOCI. We nd that many types of noise sources and the nonlinearity lead to the nonsymmetrical PDF. For the reason, the mean value shows some shift from a zero value. Moreover, it is noticed that the mean and variance values of the PDF are obtainable with the knowledge of the $\chi^2$ distribution.

## References


[1] Glenn E. Healey and Raghava Kondepudy, 1994. Radiometric CCD Camera Calibration and Noise Estimation. In:*IEEE Trans. on Pattern Analysis and Machine Intelligence*, Vol. 16, No.3, pp. 267-276.

[2] G. Amelio and G. Smith, 1970, Experimental veri cation of the charge coupled device concept. In: *Bell Syst. Tech. J.*, Vol. 49, pp. 593-600.

[3] K. Ikeuchi and T. Kanade, 1989, Modelling Sensor: Towords automatic generation of object recognition program. In:*Comp. Vision, Graphics, Image Processing*, Vol. 48, pp. 50-79.

[4] Mary L. Boas, 1983, *Mathematical Methods in the Physical Science*, Wiley, pp. 701-703.

[5] http://www.stw.tu-ilmenau.de/ ff/beruf-cc/cmos/cmos-noise.pdf

[6] G.S. Kang, 2007, GOCI Sensor Math Model, In:*GOCI CDR Datapackage*.

[7] Carl W. Helsotrom, 1984, *Probability and Stochastic Process for Engineers*, Maxwell Macmillan.


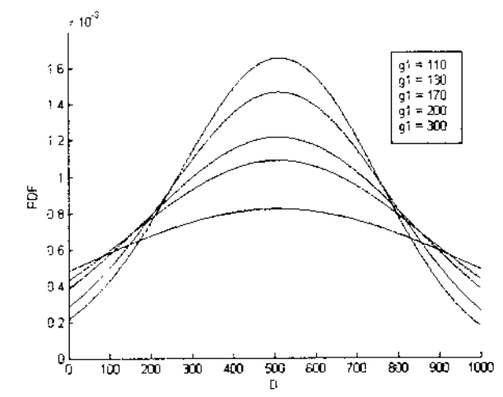


(a) PDF with $g_1$ variation: $g_2 = 1$.

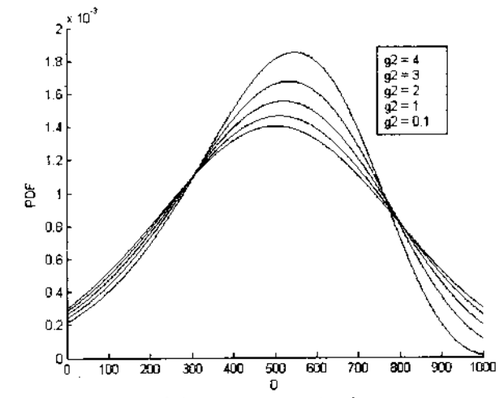


(b) PDF with $g_2$ variation: $g_1 = 170$.

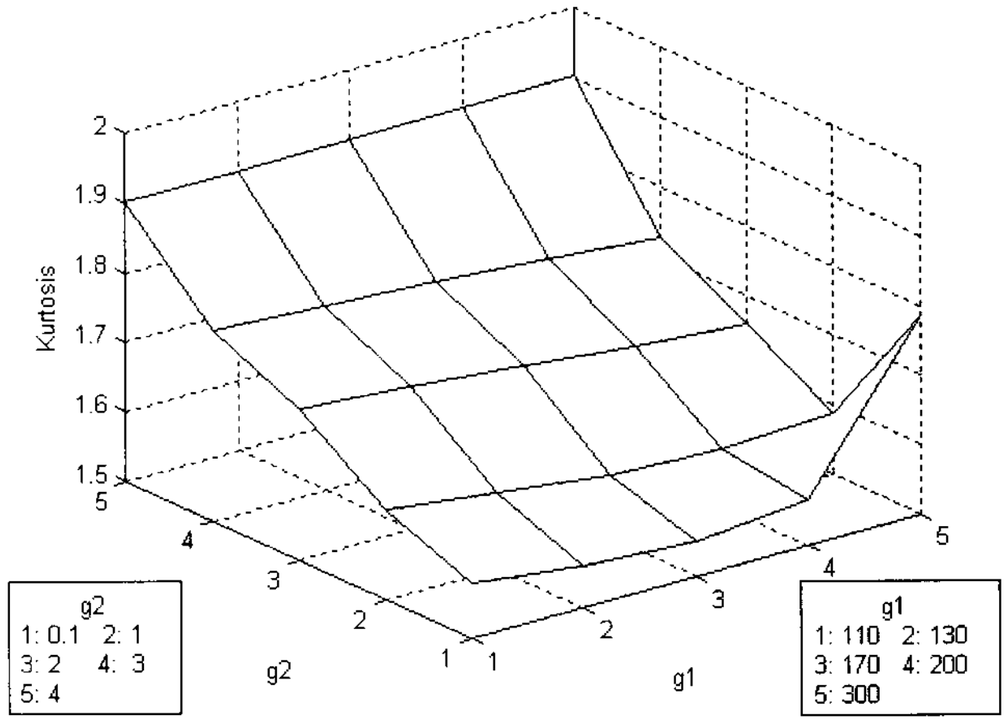


(c) Kurtosis with $g_1$ and $g_2$ variation.

Fig. 1. Relation between PDF and Gains: $D_{av} = 500$, $O_E = 1$, $\tau^2 = 1$, $q = 0.7$.

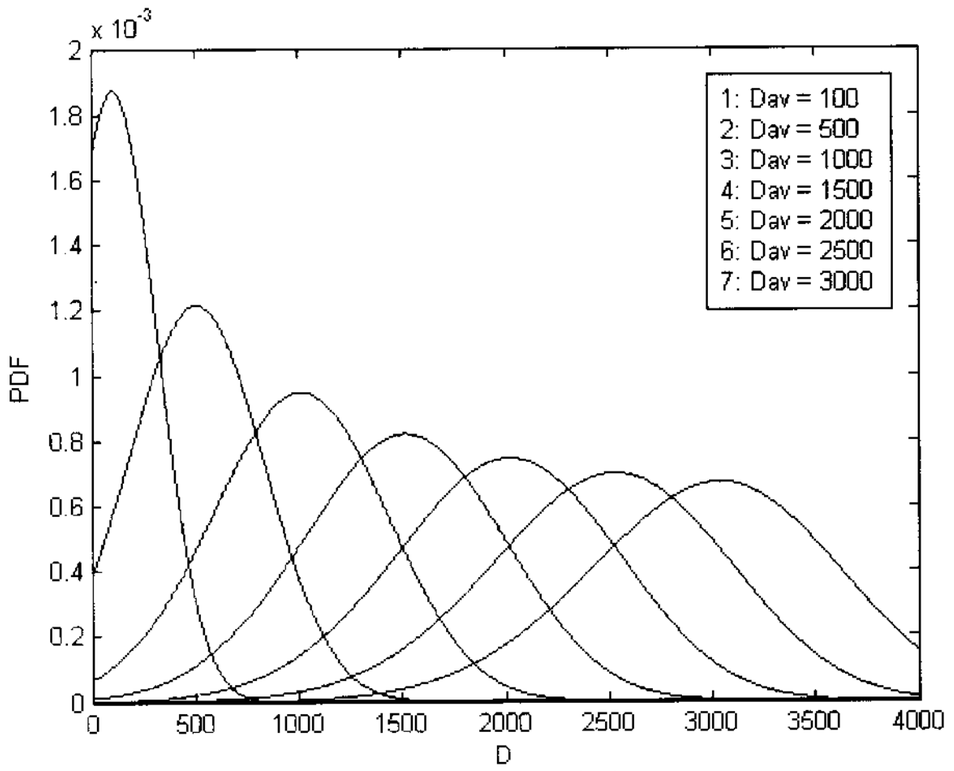


(a) PDF with $D_{av}$ variation.

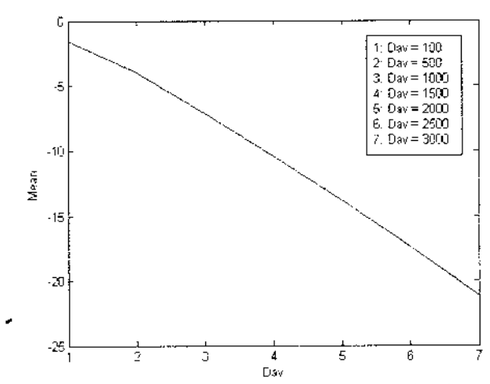


(b) Mean value with $D_{av}$ variation.

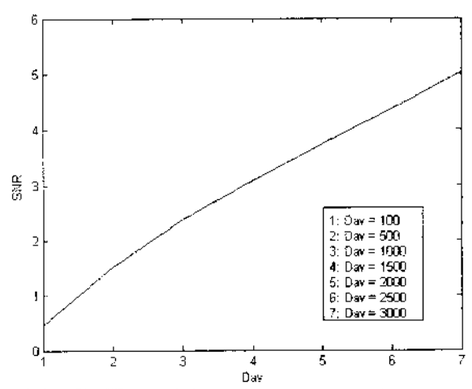


(c) SNR with $D_{av}$ variation.

Fig. 2. Relation between PDF and $D_{av}$: $g_1 = 170$, $g_2 = 1$, $O_E = 1$, $\tau^2 = 1$, $q = 0.7$.